Journal of Sound and Vibration 326 (2009) 123–136

Contents lists available at ScienceDirect

Journal of Sound and Vibration

journal homepage: www.elsevier.com/locate/jsvi

Moving follower rest design using vibration absorbers for ball screw grinding

C.C. Cheng *, C.P. Kuo, F.C. Wang, W.N. Cheng

Department of Mechanical Engineering, National Chung Cheng University, Chia-Yi 621, Taiwan, ROC

ARTICLE INFO

Article history:
Received 25 November 2008
Received in revised form
25 March 2009
Accepted 21 April 2009
Handling Editor: L.G. Tham
Available online 20 May 2009

ABSTRACT

A novel design of follower rest used in ball screw grinding machine is proposed. Installed on the grinding wheel holder and moving along the ball screw, the follower rest is designed to be a vibration absorber with its driving point attached on the ball screw close to the grinding zone. It is used not only to suppress the ball screw vibration at the position close to the grinding zone but also to avoid the occurrence of chatter. It provides an auxiliary in counteracting the ball screw vibration during a grinding process besides the traditional steady rest fixed on the machine bed. The mechanisms in ball screw vibration reduction as well as in avoiding the chatter using the absorber are formulated and studied using the impedance method. Influences of design parameters of the absorber, i.e. the absorber mass and the absorber damping, on the chatter and the transient response of the ball screw are examined in detail. Results show that increasing the mass of the absorber is the most effective way with respect to vibration reduction at the grinding position as well as avoiding the chatter. On the other hand, the absorber damping has a negative effect both on the vibration reduction of ball screw and avoiding the chatter because it reduces the driving point impedance of absorber at resonance, which is contrary to the structural damping of the ball screw that has a positive effect in avoiding the chatter. Moreover the absorber damping has little influence on the frequency bandwidth in which the ball screw vibration is suppressed by the absorber.

1. Introduction

The grinding wheel used in the ball screw grinding possesses a certain degree of imbalance and deviation in roundness due to material inhomogeneity and manufacturing tolerance. Even for a carefully balanced grinding wheel, the imbalance and the deviation from a perfect circle increase due to the wear of abrasive in a grinding process. This imbalance and/or lack of roundness cause severe ball screw vibration and then results in undesirable surface roughness on the ball screw. Furthermore, chatter may occur and the machining process becomes unstable due to the regeneration of waviness on both sides of the chip surface.

In order to suppress the excessive vibrations caused by the grinding wheel especially on a long ball screw, steady rest supports are utilized as shown in Fig. 1. They are fixed on the machine bed and distributed periodically along the ball screw. The installation of these supports is time-consuming especially when one needs to change the ball screw with a different length. Moreover, from the energy point of view, the vibration power from the grinding wheel is transferred to the machine through the steady rest instead of dissipating it and thus one may expect that the grinding machine vibration may increase.

* Corresponding author. Tel.: +5 2720411 33313; fax: +5 2720589.
E-mail address: imeccc@ccu.edu.tw (C.C. Cheng).

0022-460X/$ - see front matter © 2009 Elsevier Ltd. All rights reserved.
doi:10.1016/j.jsv.2009.04.029

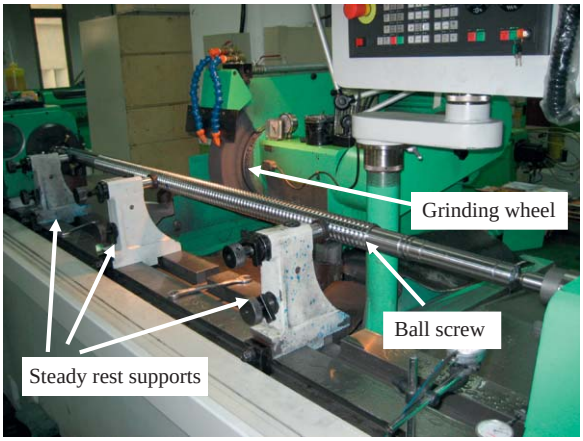

Fig. 1. Steady rest supports used in the ball screw grinding process.

In this paper, an alternative ball screw support made of vibration absorber is introduced. The dynamic vibration absorber is a traditional but effective device to reduce the undesired vibration of a machine [1–4]. Generally, the absorber can be regarded as a spring–mass–damper (SMD) system and has its best performance in vibration reduction when the excitation frequency coincides with its natural frequency. That is, the SMD creates a vibration node on the location which the SMD is bonded onto. Under this circumstance, the machine vibration can be reduced due to the node acting as a fixed support for the machine. On the other side, the SMD possesses most of the vibration power and avoid it flowing into the machine. Therefore this SMD acts as a vibration power absorber.

Based on the well-known vibration absorber technique, a novel design of ball screw follower rest is proposed. The follower rest is designed to be a SMD installed on the grinding wheel holder; and its free end or driving point is attached to the ball screw at the location close to the grinding zone. The natural frequency of the SMD is tuned to be the same as the rotational speed of the grinding wheel. Therefore the SMD would theoretically create a node on the ball screw and then acts like a fixed support. Moreover, the proposed SMD installed on the grinding wheel holder is moving with the grinding wheel assembly during the grinding process. Under this circumstance, a moving node created by the vibration absorber acts like a follower rest to effectively reduce the ball screw vibration near the grinding zone. As compared to the steady rest supports fixed on the machine bed, the proposed follower rest has a much simpler mechanism.

The rotational speed of the grinding wheel varies during a grinding process due to the fluctuation of friction force and the coupling force interacted with the ball screw [5]. However, it is well known that the frequency range for a vibration absorber is small and it depends on the mass of the vibration absorber as compared to that of the machine [1]. A vibration absorber with a wide frequency range is preferred in order to deal with situations that the rotational speed of grinding wheel might drift around the nominal value. One may use a heavier absorber to increase the operating frequency range; however, the weight and the size of a vibration absorber are always limited in the design. How to design a vibration absorber to act as a follower rest in a ball screw grinding machine and how it performs not only in suppressing the ball screw vibration but also in avoiding the occurrence of chatter will be addressed in this paper.

The first part of the paper introduces the mechanism of the vibration reduction as well as avoiding the chatter using the vibration absorber on the ball screw from the point of view of mechanical impedance. The second part focuses on quantifying the vibration reduction caused by the vibration absorber on a ball screw. The third emphasizes how to avoid chatter by using the same moving vibration absorber. Finally the available frequency range and the performance in vibration reduction as well as chatter suppression of the proposed follower rest are examined in detail.

2. Impedance of vibration absorber

Consider a SMD of mass M_a, damping constant C_a and spring constant K_a subjected to a pure tone excitation $F_2 e^{j\omega t}$ as shown in Fig. 2, in which $X_1 e^{j\omega t}$ is the displacement of the mass and $X_2 e^{j\omega t}$ is the displacement of free end. The dynamic stiffness of the SMD at the driving point is expressed as

$$\frac{F_2}{X_2} = -M_a\omega^2 \frac{1 + 2j\zeta_a r_a}{(1 - r_a^2) + 2j\zeta_a r_a}, \tag{1}$$

where ω is the excitation frequency, $\zeta_a = C_a/2\sqrt{M_a K_a}$ the damping ratio, $r_a = \omega/\omega_a$ the frequency ratio and $\omega_a = \sqrt{K_a/M_a}$ the natural frequency of SMD. The driving point impedance Z_a of the SMD is given by

$$Z_a = j\omega M_a H_a, \tag{2}$$

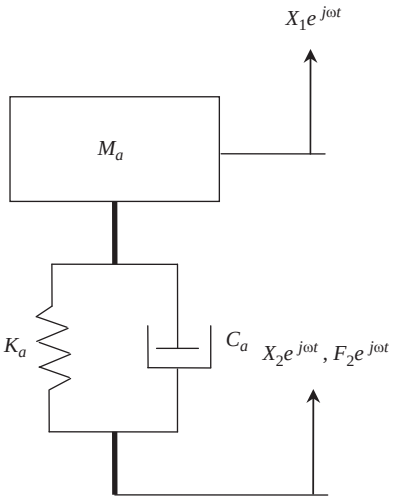

Fig. 2. SMD subjected to a harmonic force.

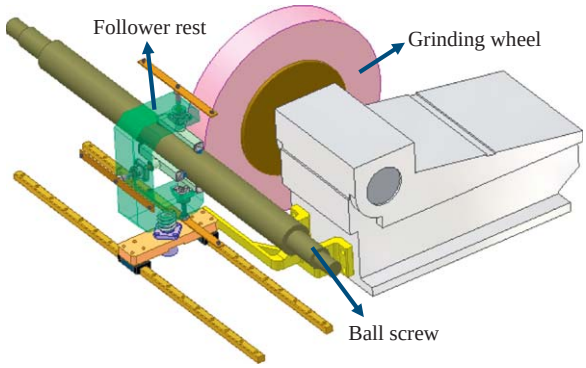

Fig. 3. A conceptual design of the follower rest using vibration absorber.

where $H_a = 1 + j2\zeta_a r_a/((1 - r_a^2) + j2\zeta_a r_a)$ denotes the displacement transmissibility [1]. Eq. (2) reveals that the driving point impedance of SMD reaches its maximum when $r_a = (1/2\zeta_a)(\sqrt{1 + 8\zeta_a^2} - 1)^{1/2}$ for $0 < \zeta_a < 1$. It implies that the driving point behaves as a node when the excitation frequency is close to the natural frequency of SMD. Based on this characteristic, a SMD is proposed to be installed on the grinding wheel head with its driving point attached onto a ball screw close to the grinding zone as illustrated schematically in Fig. 3. By tuning its natural frequency close to the excitation frequency, the SMD will behave as a vibration absorber, and a node will be created on the ball screw. This node will act as a fixed support close to the grinding zone for holding the ball screw during the grinding process. The driving point or attached position of the SMD on the ball screw is arranged to be close to the grinding zone, so the ball screw will enjoy less vibration near the grinding zone. Thus the surface roughness of the ball screw theoretically will be improved. Notice that the SMD is installed on the grinding wheel head, so the node created by this SMD on the ball screw moves with the grinding wheel during the grinding process. Under this circumstance, the SMD provides a moving, or a follower rest for the ball screw as compared to the traditional steady rest fixed on the machine bed. It is worthy of note that the ball screw bending rigidity is strengthened by this follower rest, so another intention here is to use the same follower rest to avoid the occurrence of chatter during a grinding process. Nevertheless, the effectiveness of the proposed follower rest on the ball screw vibration reduction as well as in avoiding the chatter depends, respectively, on the vibration characteristics of the SMD, the ball screw, the grinding wheel and their dynamic couplings.

3. Ball screw impedance and its coupling with vibration absorber

A physical model for a ball screw with a vibration absorber is illustrated in Fig. 4. The ball screw is modeled as a unrotating Euler–Bernoulli beam due to its slenderness and small rotational speed, e.g. 30–45 rev/min. For a ball screw without the vibration absorber subjected to a harmonic force $F_g e^{j\omega t}$ simulated as the grinding wheel at the position x_f, the

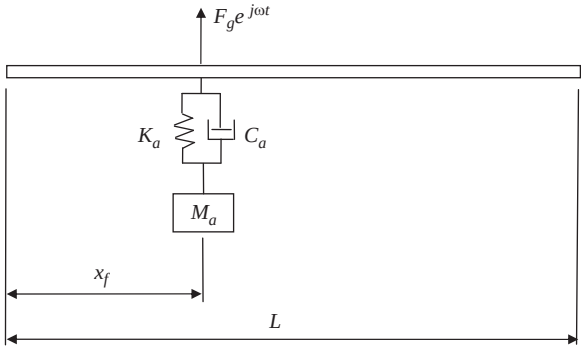

Fig. 4. Schematic diagram for a ball screw with a follower rest.

equation of motion is given by

$$EI\frac{\partial^4 w_b}{\partial x^4}+\rho A\frac{\partial^2 w_b}{\partial t^2}=F_g\delta(x-x_f)\mathrm{e}^{\mathrm{j}\omega t}, \tag{3}$$

where w_b is the ball screw transverse displacement, ω the grinding wheel rotational speed, E the Young's modulus, I the area of moment of inertia, ρ the density and A the cross-sectional area of the ball screw. Notice that the excitation frequency for the ball screw caused by the grinding wheel is assumed to be the same as the grinding wheel rotational speed due to the grinding wheel imbalance and/or lack of roundness in a machining process. Based on the mode-summation method, the vibration displacement of the ball screw, w_b can be determined straightforward:

$$w_b(x,t)=\sum_{i=1}^{N_b}\frac{\phi_i(x_f)\phi_i(x)}{EI\int_0^L\phi_i''''(x)\phi_i(x)\,\mathrm{d}x-\rho A\omega^2\int_0^L\phi_i^2(x)\,\mathrm{d}x}F_g\,\mathrm{e}^{\mathrm{j}\omega t}, \tag{4}$$

where L is the ball screw length, $\phi_i(x)$ the ith mode shape of the ball screw, the prime is the derivative with respect to x, N_b the total participating mode number. With Eq. (4), the driving point impedance for the ball screw at the grinding position can be obtained, $Z_b=F_g\,\mathrm{e}^{\mathrm{j}\omega t}/\dot{w}_b(x_f,t)$. For a ball screw with its both ends simply supported as an example, the driving point impedance is expressed as

$$Z_b=-\mathrm{j}\omega M\left\{\sum_{i=1}^{N_b}\frac{2\sin^2\left(\dfrac{\mathrm{j}\pi x_f}{L}\right)}{\left(\dfrac{1}{r_i}\right)^2-1}\right\}^{-1}, \tag{5}$$

where $M=\rho AL$ is the ball screw mass and r_i represents the frequency ratio between the excitation frequency to the natural frequency of the ith bending mode of ball screw.

For a ball screw coupled with a vibration absorber modeled as a SMD, the driving point impedance Z_{ba} at the grinding position is obtained by coupling the impedance of SMD, Z_a with that of the ball screw, Z_b based on the conditions of force equilibrium and velocity compatibility [3]:

$$Z_{ba}=Z_b+Z_a. \tag{6}$$

Fig. 5 illustrates a schematic model of the interaction between three subsystems, i.e. ball screw, grinding wheel and SMD, respectively. And the driving impedance Z_{ba} is expressed as

$$Z_{ba}=-\mathrm{j}\omega M(H_b-M_rH_a), \tag{7}$$

where $M_r=M_a/M$ is the mass ratio between the SMD mass to the ball screw mass and H_b the dynamic compliance for the ball screw at the coupling position. If the cutting impedance $Z_c=-\mathrm{j}K_c/\omega+C_c$ and the grinding wheel impedance $Z_g=\mathrm{j}(M_g\omega-K_g/\omega)+C_g$ are all taken into consideration, the mechanical analogy corresponding to the coupling system shown in Fig. 5 is illustrated in Fig. 6, where K_c is the cutting stiffness, C_c the corresponding damping, M_g, K_g and C_g are the grinding wheel mass, stiffness and damping, respectively. Notice that the processing damping C_c and stiffness K_c at the interface between the grinding wheel and machined surface are assumed to be constant for simplification, although they appears to be nonlinear in chatter vibration [6]. Eq. (7) provides a simple but straightforward relation that describes quantitatively the dynamic coupling between the ball screw and the SMD, whereas the mechanical analogy as shown in Fig. 6 offers an interpretation of the influence of SMD on ball screw vibration qualitatively. From Eq. (7), the impedance Z_{ba} becomes extremely large when H_a goes unbounded, which occurs as the natural frequency of SMD is tuned to be the same as the excitation frequency. Under this circumstance, the ball screw transverse velocity at the grinding position, $x=x_f$ almost vanishes. It is more obvious from Fig. 6 that the analogous current, i.e. the dynamic chip thickness $h(t)$ from the grinding

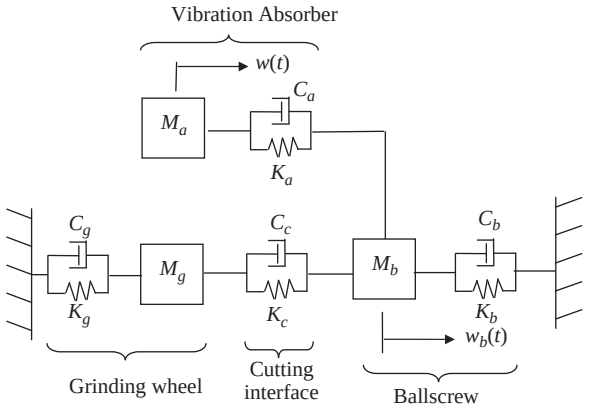

Fig. 5. Dynamic couplings between ball screw, moving support and grinding wheel.

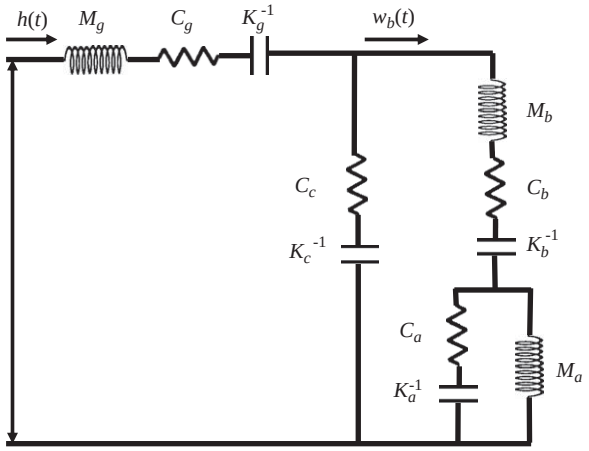

Fig. 6. Mechanical analogy of cutting stiffness, ball screw and moving support.

wheel goes to the cutting impedance completely instead of the ball screw, i.e. $w_b(x_f,t)\cong 0$ while the SMD has an infinite mechanical impedance. As a consequence, $h(t)=h_0(t)$, where h_0 is the feed per revolution or static chip thickness [7].

4. Vibration absorber and chatter

Avoiding the machining instability, i.e. the chatter, is always an important issue for a metal grinding process. The regeneration of waviness on the ball screw or/and grinding wheel causes the dynamic orthogonal cutting equation to be a delayed differential equation, i.e. $h(t)=h_0-w_b(t)+\mu w_b(t-T)$, where μ is the overlap factor, T the rotation period of the workpiece, $w_b(t)$ and $w_b(t-T)$ are the present and past vibration amplitudes of the ball screw in the radial direction, respectively. The transfer function which defines the ratio between the general dynamic chip thickness $h(t)$ and the static chip thickness $h_0(t)$ after Laplace transform is given by [7]

$$\frac{h(s)}{h_0(s)}=\frac{1}{1+(1-\mu e^{-Ts})\dfrac{Z_{gc}}{Z_{ba}}}, \tag{8}$$

where $Z_{gc}=Z_g+Z_c$ and the chatter loop using block diagrams is depicted in Fig. 7(a). For a further investigation, Eq. (8) is rewritten as

$$\frac{h(s)}{h_0(s)}=\frac{1}{1-G/G_{CP}}, \tag{9}$$

where $G_{CP}(\mu,T)=-1/(1-\mu e^{-j\omega T})$ and $G=Z_{gc}/Z_{ba}$. The machine becomes stable, critical stable or unstable depending on the roots of denominator. Consider a simply supported ball screw with Young's modulus $E=200\,\text{GPa}$, density $\rho=7700\,\text{kg/m}^3$, length $L=2\,\text{m}$ and diameter $d=0.05\,\text{m}$. Assume that the grinding wheel has a mass twice as large as the

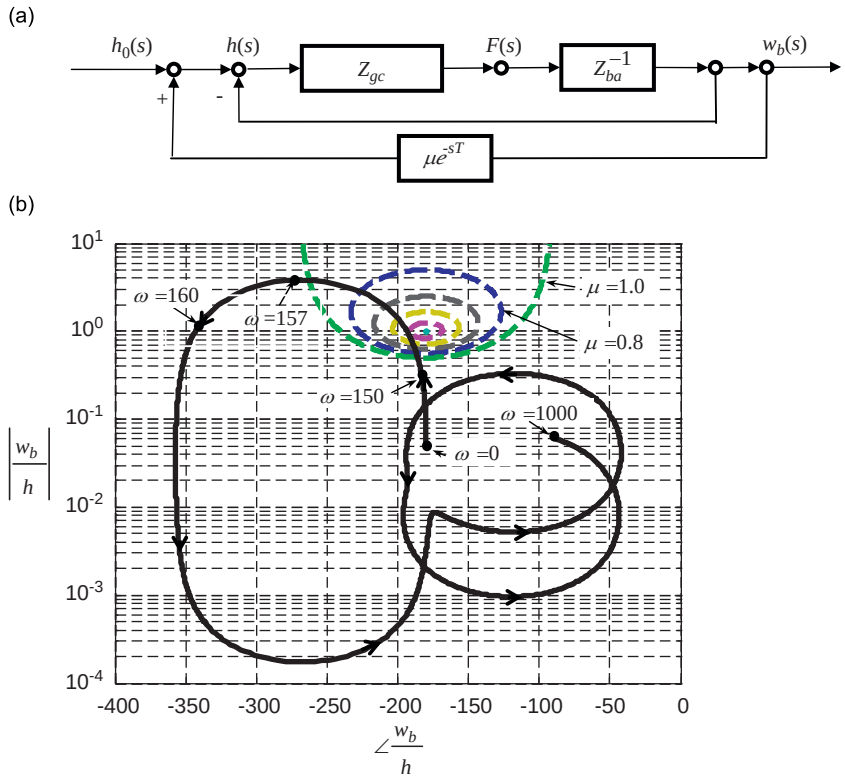

Fig. 7. (a) Block diagram of conventional chatter loop and (b) gain–phase plot of ball screw without follower supports.

ball screw, i.e. $M_g = 2M$ and its stiffness and damping are the same as those of the cutting interface, i.e. $K_c = K_g = 2 \times 10^7$ N/m, $C_g = C_c = 2.6 \times 10^3$ N s/m. A gain–phase plot, i.e. the Merritt curve [8], of the ball screw without absorber as a follower support is shown in Fig. 7(b). In this figure, varying the rotational speed of ball screw, the locus of G_{CP} is denoted by the dotted line whereas G is represented by the solid line. The locus of G appears to be multiple ellipses with each representing a dominating vibration mode of ball screw starting from $\omega = 0$ to 1000 rad/s in a direction indicated by the arrow. For example, the apex of the ellipse which occurs at $\omega = 157$ rad/s has a maximal value of $|w_b/h| = 3$ due to the first resonance of ball screw. Note that the chatter occurs when the denominator of Eq. (9) goes to zero, which is represented graphically by the intersections between the loci of G_{CP} and G. It implies that the chatter can be avoided if the loci of G which is controlled by Z_{gc}/Z_{ba} can be moved away from those of G_{CP}. That is, changing the impedance Z_{ba} by tuning the absorber impedance Z_a, the loci of G may not intersect that of G_{CP}. Under this circumstance, the chatter will not occur and the machine becomes more stable even it is operated at a high cutting speed for a better efficiency. To accomplish this task, theoretically the ball screw with absorber needs to have infinite impedance at the cutting position, i.e. $Z_{ba} \to \infty$ or the absorber should have an infinite impedance, i.e. $Z_a \to \infty$, which reaches the same conclusion as to reduce the ball screw vibration near the grinding position. Therefore the goal of implement of an absorber as a moving follower rest is not only to suppress the vibration near the grinding position but also to avoid the chatter.

5. Transient vibration analysis of ball screw with follower rests

In the previous section, the mechanism of vibration reduction and avoidance of chatter using the vibration absorber on the ball screw was examined qualitatively from the point of view of mechanical impedance. The question now is how to quantify the effect of vibration reduction with and without the moving vibration absorber installed on the ball screw. To address this issue, a transient vibration analysis of ball screw with and without a moving vibration absorber is presented in this section. Consider again the physical model of a ball screw and a moving absorber as illustrated in Fig. 4. The proposed ball screw follower rest is simplified as a spring–mass–damper system and is moving with the grinder head. The grinding force acting on the ball screw from the grinding wheel includes a moving transverse force $F_g e^{j\omega t}$ and a moving longitudinal force S due to friction. The equation of motion for the ball screw is expressed as

$$EI\frac{\partial^4 w_b}{\partial x^4} - S\frac{\partial^2 w_b}{\partial x^2} + \rho A\frac{\partial^2 w_b}{\partial t^2} = (F_g e^{j\omega t} + F_T)\delta(x - V_0 t), \tag{10}$$

where w_b is the ball screw displacement and V_0 the moving speed of grinding wheel holder along the ball screw. Notice that the vibration absorber is attached on the grinder head, so it moves with the same speed as the grinding wheel holder. The external force acting on the ball screw consists of three components: the transverse force directly from the grinding wheel F_g, the feed back force from the SMD, $F_T = \omega^2 M_a H_a w_b$ and the frictional force caused by the grinding wheel, $S = F_g \mu_f$, where μ_f is the friction coefficient. Substituting F_T into Eq. (10), the equation of motion for the ball screw with a moving absorber is rewritten as

$$EI\frac{\partial^4 w_b}{\partial x^4} - S\frac{\partial^2 w_b}{\partial x^2} + [\rho A + M_a H_a \delta(x - V_0 t)]\frac{\partial^2 w_b}{\partial t^2} = F_g \delta(x - V_0 t)\mathrm{e}^{\mathrm{j}\omega t}. \tag{11}$$

Based on the mode-summation method, the assumed displacement, $w_b(x,t) = \sum_{m=1}^{N} C_m(t)\phi_m(x)$ of the ball screw is substituted into Eq. (11):

$$EI\sum_{m=1}^{N} C_m(t)\phi_m''''(x) - S\sum_{m=1}^{N} C_m(t)\phi_m''(x) + [\rho A + M_a H_a \delta(x - V_0 t)]\sum_{m=1}^{N} C_m(t)\phi_m(x) = F_g \delta(x - V_0 t)\mathrm{e}^{\mathrm{j}\omega t}, \tag{12}$$

where C_m the modal coefficient corresponding to mth mode shape function $\phi_m(x)$ that satisfies associated boundary conditions, e.g. $\phi_m(x) = \sin(m\pi x/L)$ for pinned–pinned boundary conditions. N is the total participating mode number and 10 modes, i.e. $N = 10$ are assumed to participate in the simulation of this study. Multiplying Eq. (12) by $\phi_n(x)$ and integrating it from 0 to L, Eq. (12) is written as

$$\mathbf{M}\ddot{\mathbf{C}} + \mathbf{K}\mathbf{C} = \mathbf{F}, \tag{13}$$

where $\mathbf{M} = [m_{ij}]$, $m_{ij} = \rho A \int_{x=0}^{L} \phi_i^2(x)\,\mathrm{d}x\delta_{ij} + M_a H_a \phi_i(V_0 t)\phi_j(V_0 t)$, $\mathbf{K} = [k_{ij}]$, $k_{ij} = [EI \int_{x=0}^{L} \phi_i''''(x)\phi_i(x)\,\mathrm{d}x - S\int_{x=0}^{L} \phi_i''(x)\phi_i(x)\,\mathrm{d}x]\delta_{ij}$, $\mathbf{F} = \{f_1, f_2, \ldots, f_i, \ldots, f_N\}^{\mathrm{T}}$, $f_i = F_g \phi_i(x = V_0 t)\mathrm{e}^{\mathrm{j}\omega t}$, $\mathbf{C} = \{C_1(t), C_2(t), \ldots, C_N(t)\}^{\mathrm{T}}$, where the matrix and the vector are represented by boldfaced letters. Eq. (13) can be solved by introducing state vectors $\mathbf{y} = \{\mathbf{C}, \dot{\mathbf{C}}\}^{\mathrm{T}}$ into Eq. (13):

$$\dot{\mathbf{y}} = \mathbf{A}(t)\mathbf{y} + \tilde{\mathbf{F}}(t), \tag{14}$$

where

$$\mathbf{A}(t) = \begin{bmatrix} \mathbf{0} & \mathbf{I} \\ -\mathbf{M}^{-1}\mathbf{K} & \mathbf{0} \end{bmatrix}$$

and $\tilde{\mathbf{F}}(t) = \{\mathbf{0}, \mathbf{M}^{-1}\mathbf{F}\}^{\mathrm{T}}$. The transient vibration response of the ball screw can be obtained as the coefficient $\mathbf{C}$ is determined by solving Eq. (14) using Runge–Kutta–Fehlberg method [9]. Once the transient vibration response of the ball screw is obtained, one may quantify influence of the moving absorber on the ball screw vibration, which is described in the following section.

6. Vibration simulation of ball screw with proposed follower rests

Consider a simply supported ball screw with Young's modulus $E = 200$ GPa, density $\rho = 7700\,\mathrm{kg/m^3}$, length $L = 2$ m and diameter $d = 0.05$ m, i.e. the length–diameter ratio is $L/d = 40$. The dimensionless ball screw deflections γ at position R_x, the moving absorber speed V_r, the mass of absorber M_r, the damping ratio ζ_a, the grinding wheel position R_f and its rotational speed ω_r are defined as follows:

$$\omega_r = \frac{\omega}{\omega_{1\mathrm{EB}}}, \quad \gamma = \frac{w_b}{w_s}, \quad R_x = \frac{x}{L}, \quad R_f = \frac{x_f}{L}, \quad V_r = \frac{V_0}{V_{\mathrm{cr}}}, \tag{15}$$

where x_f is the grinding force location, $V_{\mathrm{cr}} = (\pi/L)\sqrt{EI/\rho A}$ the fundamental critical speed of a pinned–pinned, non-rotating Euler–Bernoulli beam, $\omega_{1\mathrm{EB}}$ and $w_s = F_g L^3/48EI$ are the first natural frequency and the static deflection at midspan of a pinned–pinned Euler–Bernoulli beam, respectively.

Assume that the moving absorber has a damping ratio $\zeta_a = 0.001$ and a mass ratio $M_r = 0.01$. The grinding wheel has a rotational frequency 1150 rev/min and is moving at a speed 2000 mm/min, i.e. $\omega_r = 0.77$ and $V_r = 0.33 \times 10^{-3}$, respectively. The friction coefficient μ_f is assumed to be 0.1. Fig. 8 displays the ball screw displacement response while the grinding wheel is working along the ball screw without vibration absorbers. In this figure, the horizontal axis represents the normalized ball screw position R_x, whereas the vertical axis indicates the grinding force location R_f. A slice through this figure, denoted by the horizontal dashed line for example, depicts the ball screw displacement response while the grinder is working at the midspan of the ball screw, $R_f = 0.5$. For a low excitation frequency in this example, i.e. $\omega_r = 0.77$, it is not surprising that the maximal displacement occurs at the midspan while the grinding wheel is also working at the same position, $R_f = R_x = 0.5$. Another slice denoted by the dotted line represents the ball screw driving displacement response, i.e. the response at the position of the grinding force. It shows that the ball screw response is dominated by its own first bending mode in this specific example. However, more vibration modes will involve in the ball screw vibration when the ball screw has a greater slenderness or the rotational speed of the grinding wheel increases.

To quantify the vibration reduction caused by the proposed moving absorber used as a follower rest, the normalized displacements γ of the ball screw with and without the moving absorber are illustrated in Fig. 9. It shows that the ball

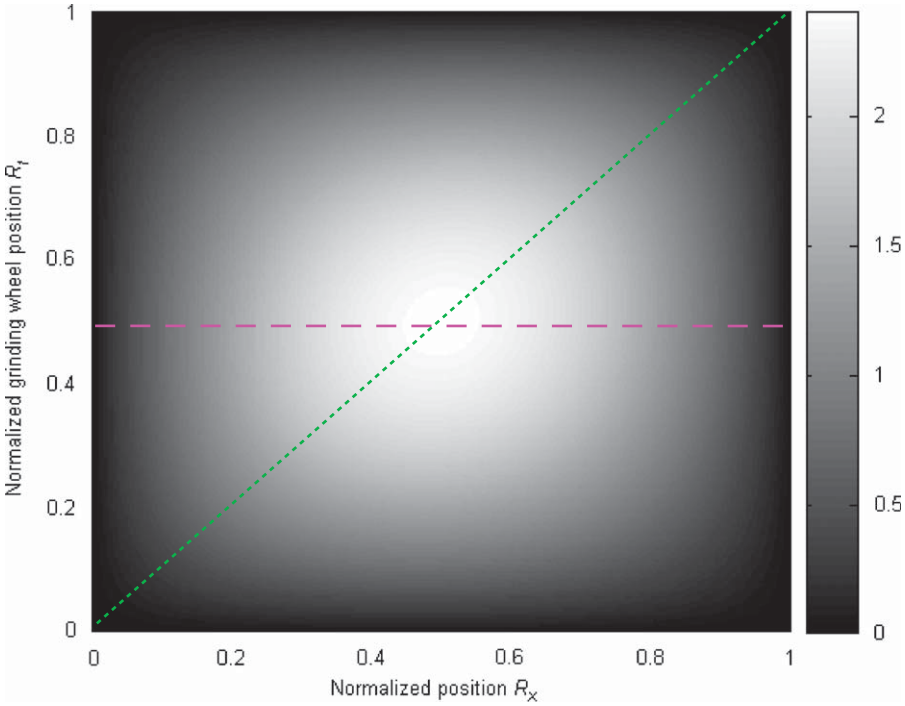

Fig. 8. Normalized displacement of ball screw without support.

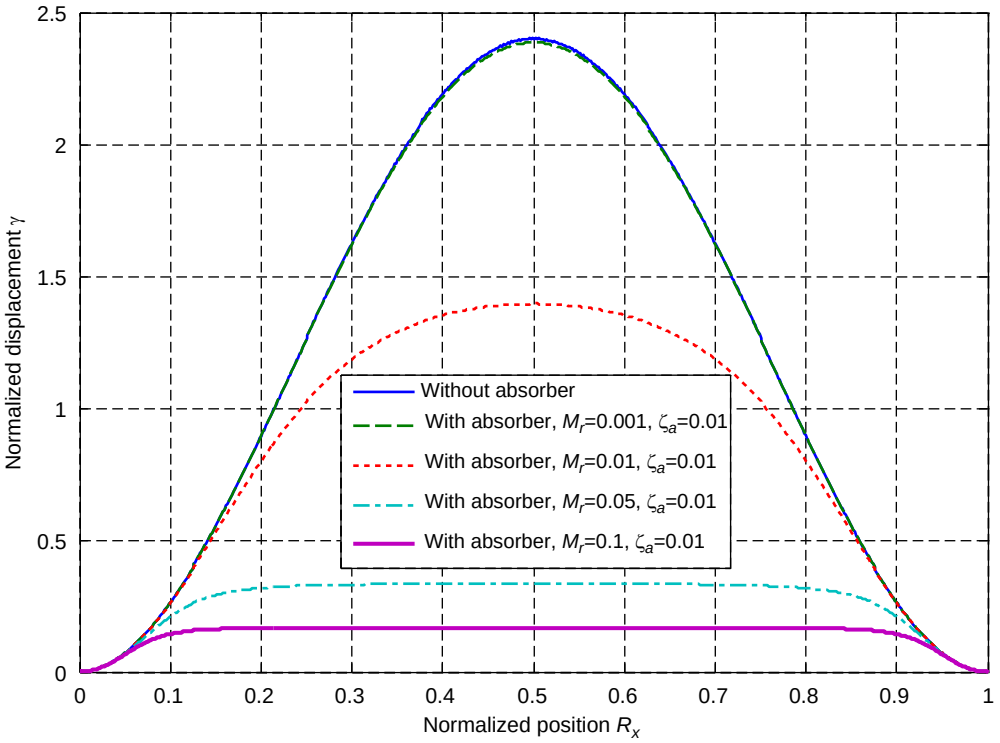

Fig. 9. Influence of absorber mass on ball screw vibration for $\zeta_a = 0.01$.

screw vibration at the grinding position is suppressed by the absorber as expected. The maximal vibration reduction is approximately 92 percent at the midspan of the ball screw for a mass ratio $M_r = 0.1$ and damping ratio $\zeta_a = 0.01$. It also shows that the moving absorber has its best performance at the midspan where the maximal displacement occurs at the

same position. As a result one may expect that the surface roughness of the ball screw caused by vibration during grinding can be much improved with the proposed follower rest.

7. Influence of absorber mass and damping on ball screw vibration

It is intuitive to have a large vibration absorber in order to have sufficient momentum to suppress the ball screw vibration. Fig. 9 confirms this statement by comparing the displacement response of the ball screw with a moving support for four different mass ratios, $M_r = 0.001$, 0.01, 0.05 and 0.1, respectively. Nevertheless the absorber is usually size-limited due to space limitation in the grinding wheel holder.

In a grinding process, the rotational speed of grinding wheel may drift due to the unsteady friction force as well as the varying transverse force caused by the ball screw vibration. Therefore it is desirable to have a vibration absorber with a wide frequency range to accommodate all the possible rotational speed drift of the grinding wheel during a grinding process. To quantify the available frequency bandwidth in which the vibration absorber is effective in suppressing the ball screw vibration, the displacement transmissibility ratio is defined as:

$$\mathrm{DT(dB)} = 10\log\left(\frac{Z_b}{Z_{ba}}\right). \tag{16}$$

Note that DT has the same physical interpretation as the ball screw displacement ratio between the ball screw with and without the moving absorber. It is obvious that the available frequency bandwidth is the frequency range in which the displacement transmissibility ratio, DT is less than zero.

Assume that the absorber has a small damping, $\zeta_a = 0.001$ and the grinding wheel is working at the midspan of ball screw, $R_f = 0.5$. The displacement transmissibility ratio for the ball screw with a moving absorber is shown in Fig. 10 for three different mass ratios, $M_r = 0.01$, 0.05 and 0.1, respectively. From this figure, the available frequency range can be easily identified, e.g. the frequency for $M_r = 0.1$ ranges from 0.8 to $1.12\omega_a$ approximately. Notice that the trough indicated by the circle is due to the resonance of ball screw without the moving absorber. The absorber has its best performance at $r_a = 1$, i.e. the frequency at which the vibration absorber has its maximal impedance on the ball screw.

It is well known that damping has its maximal effect on the vibration response when the system is resonant. The issue needs to be addressed here is how the damping affects the frequency bandwidth as well as the performance of the moving absorber. Fig. 11 shows the displacement response for the ball screw with a moving absorber, $M_r = 0.05$ for four different damping ratios, $\zeta_a = 0.001$, 0.01, 0.05 and 0.1, respectively. It shows that the vibration reduction caused by the moving absorber decreases as the damping increases. The reason is that the impedance Z_a of the absorber decreases as the damping increases when the natural frequency of the absorber is tuned to be close to the excitation frequency. However, the

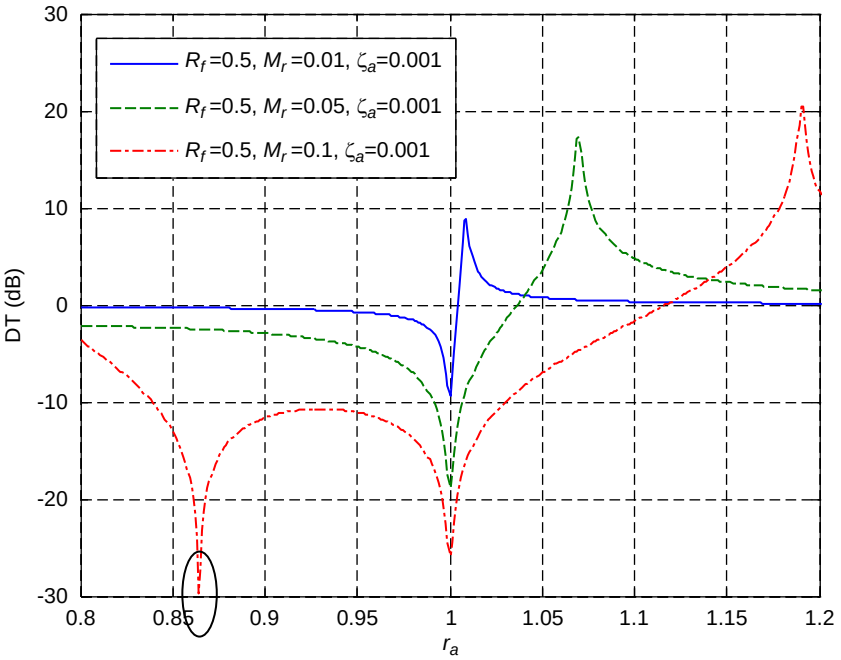

Fig. 10. Influence of absorber mass on frequency bandwidth.

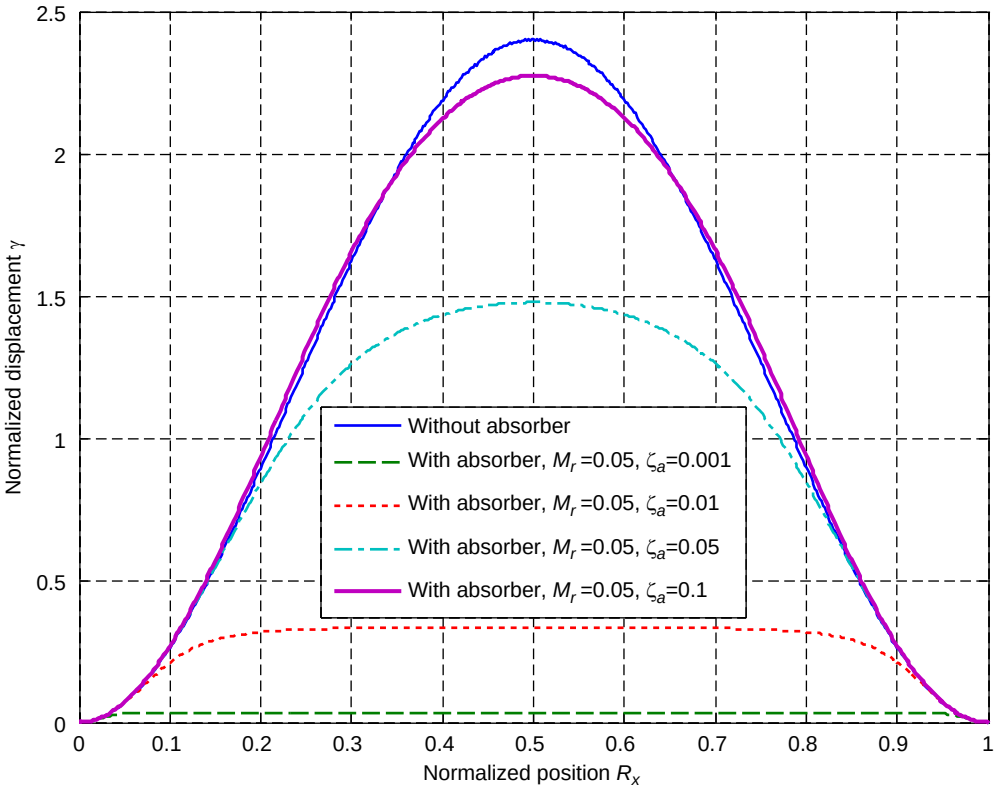

Fig. 11. Influence of absorber damping ratio on ball screw vibration.

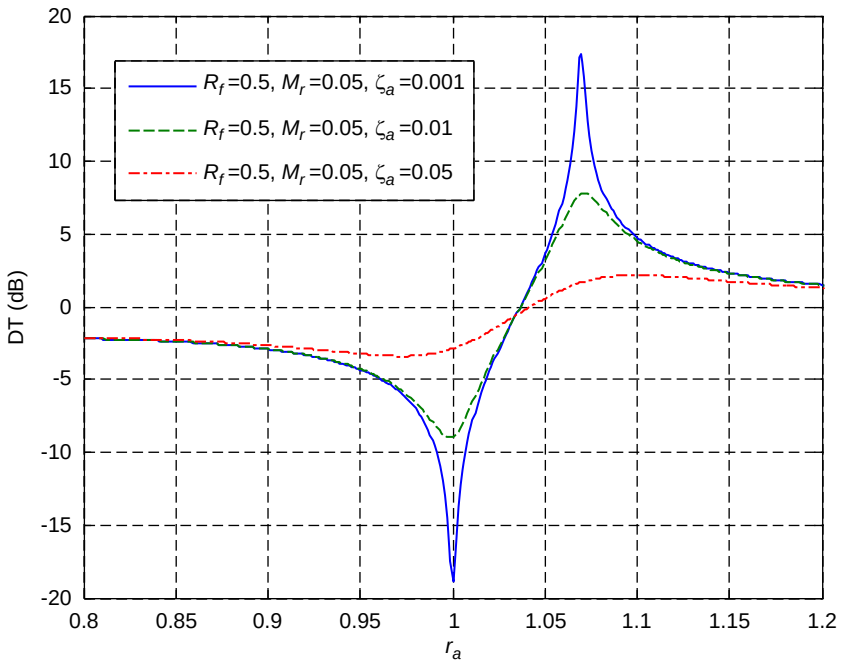

Fig. 12. Influence of damping ratio of absorber on frequency bandwidth.

damping has little influence on the frequency bandwidth as seen in Fig. 12. From Figs. 11 and 12, we conclude that a small damping for the moving absorber is desirable in order to restrain the vibration of the absorber itself without scarifying its performance in reducing the ball screw vibration too much.

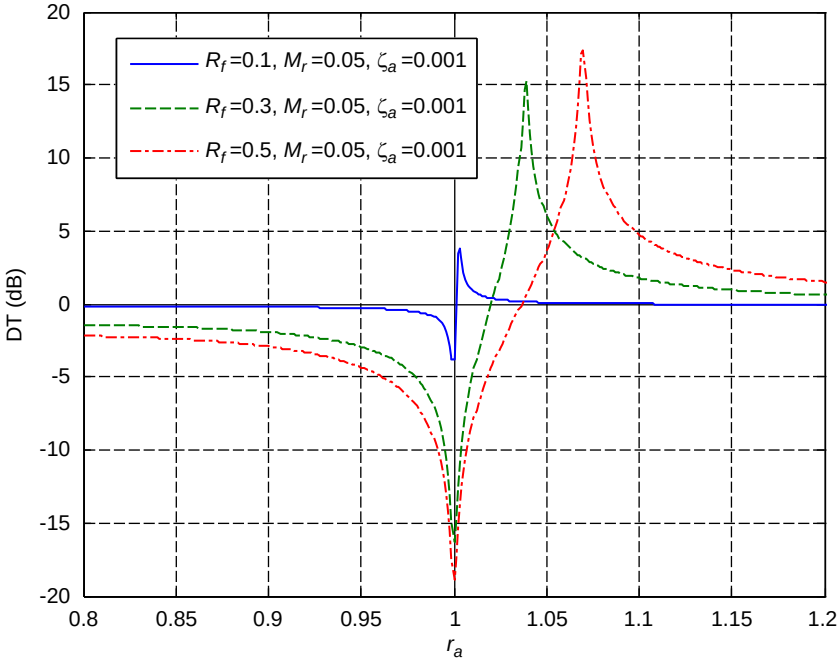

Fig. 13. Influence of absorber location on frequency bandwidth.

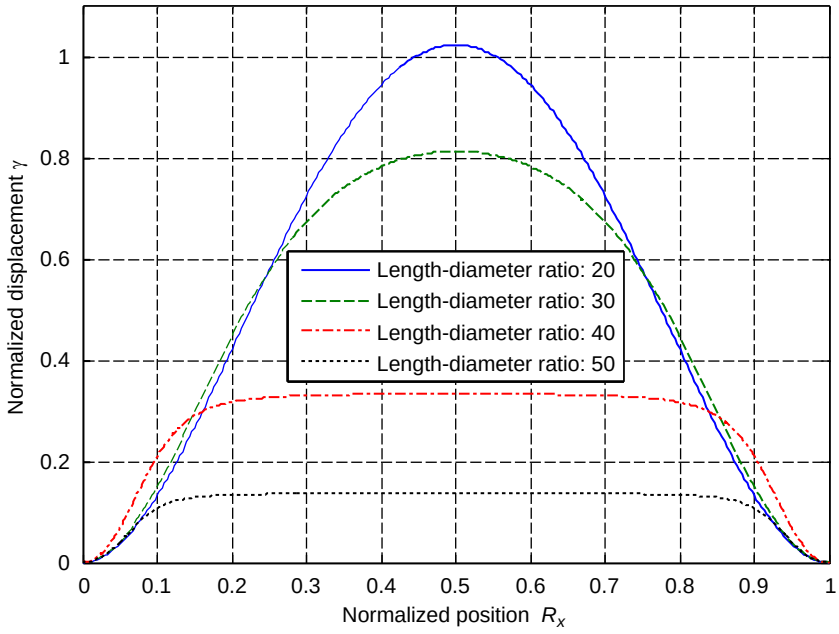

Fig. 14. Ball screw vibration displacement for varying length–diameters, $M_r = 0.05$, $\zeta_a = 0.01$.

It is worthy of note that the available frequency bandwidth also varies as the absorber and grinding wheel move along the ball screw. Fig. 13 displays the displacement transmissibility ratio for the ball screw with a moving absorber, $M_r = 0.05$ and $\zeta_a = 0.001$ while the grinding wheel is working at three different positions, $R_f = 0.1$, 0.3 and 0.5, respectively. It shows that the vibration reduction caused by the moving absorber is not sensitive to the frequency drift of the grinding wheel when the grinding force is acting at the midspan of the ball screw. On the contrary, the frequency drift may cause problems when the moving absorber is near either end of the ball screw. Nonetheless, the ball screw vibration is small as compared to that on the midspan due to the clamps at two end of the ball screw, and thus the frequency drift will not cause too much trouble when the grinding wheel is working near either end of the ball screw.

The influence of absorber mass and damping on the vibration reduction of a ball screw was examined. However, the driving point impedance Z_{ba} depends not only on the vibration absorber but also on the ball screw itself. Therefore the performance of a vibration absorber varies with respect to the ball screw of various sizes. Fig. 14 illustrates the displacement response of the ball screw with a vibration absorber for four different length–diameter ratios, $L/d = 20, 30, 40$ and 50, respectively. In this specific example, the mass and damping ratio of the absorber are assumed to be $M_r = 0.05$ and $\zeta_a = 0.01$. It is not surprising to show that the absorber enjoys a better performance in vibration reduction when the ball screw has a greater length–diameter ratio.

8. Influences of absorber mass and damping on chatter

As stated in Introduction, the goal of implementing an absorber as a moving follower rest is not only to suppress the vibration at the grinding point but also to avoid the occurrence of chatter. Fig. 15 shows the influences of absorber mass M_r on the gain–phase relationship for different values of overlap factor μ and rotational speed ω, where the damping ratio of the absorber is assumed to be 0.0001. The locus of the impedance ratio with the absorber excluded $G_b = Z_{gc}/Z_b$ varying from $\omega = 0$ to 200 rad/s is represented by the thin solid line. The chatter occurs as the locus of G_b intersects G_{CP} represented by the ellipses as discussed in Section 4. Varying the absorber mass from $M_r = 0$ to 0.3, the loci of $G = Z_{gc}/Z_{ba}$ are represented by three thick curves, denoted by the dotted, the solid, and the dash-dotted lines, for $\omega = 150$, 155 and 160 rad/s, respectively. All three curves exhibit a tendency that they move away from G_{CP} when increasing the absorber mass. Although the absorber can effectively suppress the vibration near the grinding position; however, the chatter may still occurs if the absorber mass is not large enough, e.g. $M_r < 0.001$ at $\omega = 155$ rad/s. It clearly reveals that increasing the absorber mass until $|w_b/h| \le 0.5$ can avoid the occurrence of chatter.

It is of worthy of note that the resonances occur when the system impedance vanishes, i.e. $Z_{ba} = 0$, or G becomes maximal. For example, in Fig. 7(b), the first resonance of the ball screw without absorber occurs at $\omega = 157$ rad/s (24.98 Hz). On the other hand, the time delay T can be expressed as $T = 2\pi(n+\nu)/\omega$, where n is a positive integer, i.e. $n = 0, 1, 2, \ldots$, and ν is the phase factor with a range $0 < \nu < 1$ [8]. Notice that G_{CP} can be uniquely plotted as a function of μ and ν on the Merritt's locus. As the chatter occurs, i.e. $G_{CP} = G$, or $Z_{ba} + Z_{gc}(1 - \mu e^{-j\omega T}) = 0$, the chatter frequency $\omega = \omega_{\text{chatter}}$ is determined for a specific μ. And for a given overlay μ the time delay $T = 2\pi(n+\nu)/\omega$ or the critical speed $N = 1/T$ is determined from $Z_{ba} + Z_{gc}(1 - \mu e^{-j\omega T}) = 0$.

The influence of absorber damping ζ_a on the Merritt curve is shown in Fig. 16, in which the absorber mass is assumed to be $M_r = 0.01$ and the absorber damping ζ_a varies from 0 to 0.3. It shows that increasing the damping of the absorber has a tendency to move the locus of G toward those of G_{CP} as indicated by the arrow, which is contrary to the trend of increasing the absorber mass. Recall that the impedance Z_a of the absorber decreases as the damping increases when the natural frequency of the absorber is tuned to be close to the excitation frequency as seen from Eq. (2). The value of G becomes larger as the impedance Z_{ba} decreases; therefore, increasing the absorber damping has a greater chance to induce chatter.

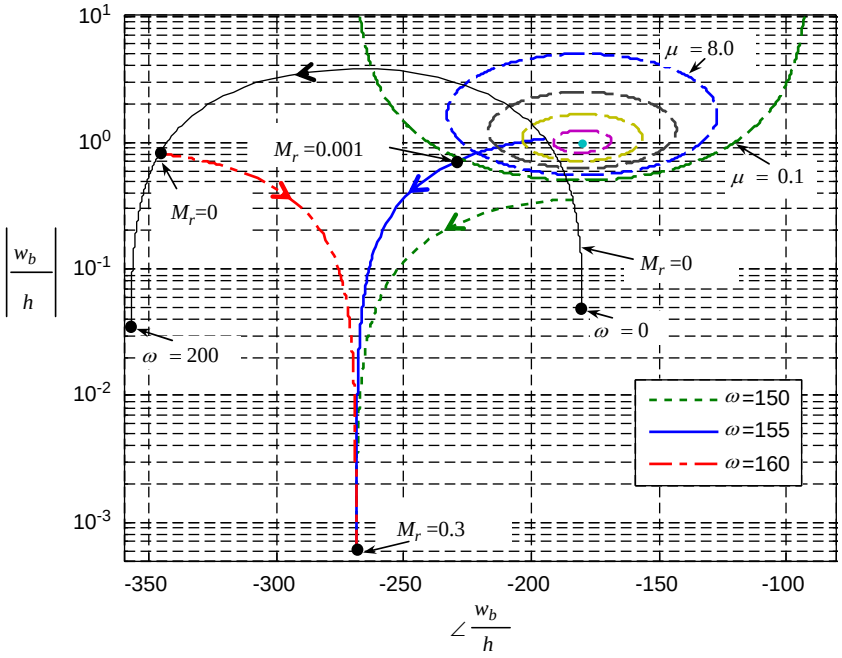

Fig. 15. Gain–phase plot of ball screw with a moving rest follower of varying mass ratio ranging from $M_r = 0$ to 0.3.

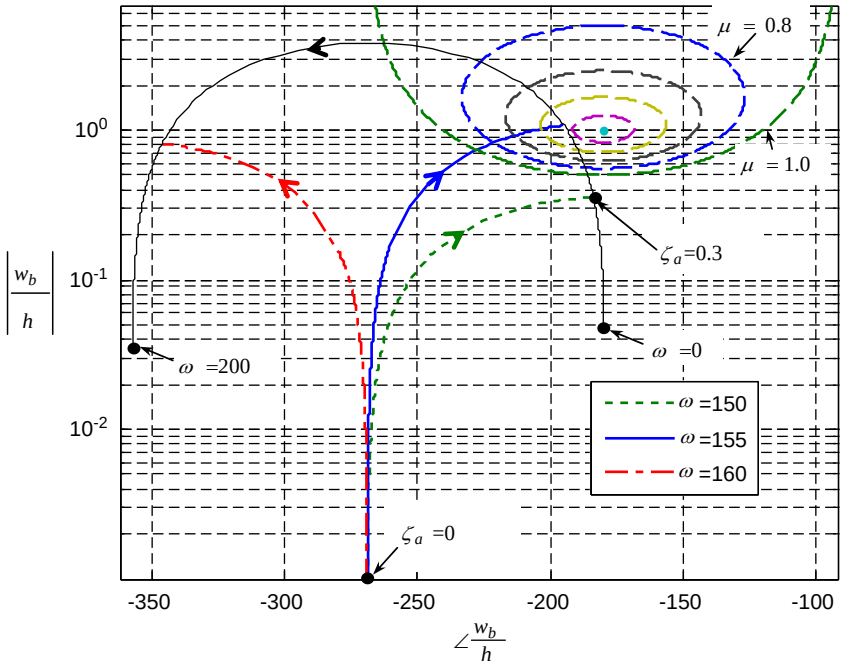

Fig. 16. Gain–phase plot of ball screw with a moving rest follower of varying damping ratio from $\zeta_a = 0$ to 0.3.

However, from Eq. (6), it is worthy of note that one may increase Z_b and Z_{ba} by increasing the structural damping of the ball screw, which is a traditional method to reduce the chance of chatter.

9. Conclusion

A novel design of follower rest used in ball screw grinding machine is proposed. Installed on the grinding wheel holder and moving along the ball screw, the follower rest is designed to be a vibration absorber with its driving point attached on the ball screw. When the natural frequency of the vibration absorber is tuned to be close to the excitation frequency, the driving point impedance of the absorber becomes extremely large. Under this circumstance, the driving point acts as a fixed support for the ball screw and then the ball screw vibration near the grinding zone can be much reduced. Furthermore, the increase of the ball screw impedance using the vibration absorber enables the ball screw to avoid the occurrence of chatter during a grinding process, which is examined using the impedance method and interpreted using the Merritt curve. Results show that increasing the mass of the absorber is the most effective way in reducing the ball screw vibration at the grinding zone, avoiding the chatter and increasing the frequency bandwidth in which the ball screw vibration is suppressed by the absorber. However, the absorber is usually size-limited due to space limitation. To quantify the proposed follower rest bandwidth, an absorber with a mass ratio $\frac{1}{10}$ has a bandwidth of 0.3Ω, where Ω is the grinding wheel rotational speed. On the contrary, the absorber damping has little influence on the frequency bandwidth. It is well known that increasing the ball screw damping is one of the methods in reducing the chance of chatter. However, increasing the damping of the absorber has a tendency to increase the possibility of chatter because it reduces the driving point impedance of absorber at resonance.

Acknowledgment

This work was partially supported by HIWIN Technologies Corp., Taiwan, Republic of China.

References

[1] S.S. Rao, *Mechanical Vibration*, Addison-Wesley, New York, 1995.
[2] S.G. Hill, S.D. Snyder, Design of an adaptive vibration absorber to reduce electrical transformer structural vibration, *Journal of Vibration and Acoustics* 124 (2002) 606–611.
[3] C.C. Cheng, P.W. Wang, Design of vibration absorbers used in multiple tonal excitations, *Journal of Vibration and Acoustics* 128 (1) (2006) 106–114.
[4] C.C. Cheng, F.T. Wu, K.L. Ho, Design and analysis of a speed-dependent torsional vibration absorber, *Journal of Automobile Engineering* 220 (6) (2006) 763–774.
[5] S.C. Salmon, *Modern Grinding Process Technology*, McGraw-Hill, New York, 1992.

[6] B.Y. Lee, Y.S. Tarng, S.C. Ma, Modeling of the process damping force in chatter vibration, *International Journal of Machine Tools & Manufacture* 35 (7) (1994) 951–962.
[7] Y. Altintas, M. Weck, Chatter stability of metal cutting and grinding, *Annals of the CIRP* 53 (2) (2004) 619–642.
[8] H.E. Merritt, Theory of self-excited machine tool chatter, *Journal of Engineering for Industry* 87 (1965) 447–454.
[9] W.H. Enright, J.D. Pryce, *Two FORTRAN Packages for Assessing Initial Value Methods*, ACM, New York, 1987.